

Original Article

Design of Light Multi-layered Shields for Use in Diagnostic Radiology and Nuclear Medicine via MCNP5 Monte Carlo Code

Mehdi Zehtabian^{1*}, Elham Piruzan¹, Zahra Molaiemanesh¹, Sedigheh Sina²

Abstract

Introduction

Lead-based shields are the most widely used attenuators in X-ray and gamma ray fields. The heavy weight, toxicity and corrosion of lead have led researchers towards the development of non-lead shields.

Materials and Methods

The purpose of this study was to design multi-layered shields for protection against X-rays and gamma rays in diagnostic radiology and nuclear medicine. In this study, cubic slabs composed of several materials with high atomic numbers, i.e., lead, barium, bismuth, gadolinium, tin and tungsten, were simulated, using MCNP5 Monte Carlo code. Cubic slabs ($30 \times 30 \times 0.05 \text{ cm}^3$) were simulated at a 50 cm distance from the point photon source. The X-ray spectra of 80 kVp and 120 kVp were obtained, using IPEM Report 78. The photon flux following the use of each shield was obtained inside cubic tally cells ($1 \times 1 \times 0.5 \text{ cm}^3$) at a 5 cm distance from the shields. The photon attenuation properties of multi-layered shields (i.e., two, three, four and five layers), composed of non-lead radiation materials, were also obtained via Monte Carlo simulations.

Results

Among different shield designs proposed in this study, the three-layered shield, composed of tungsten, bismuth and gadolinium, showed the most significant attenuation properties in radiology, with acceptable shielding at 140 keV energy in nuclear medicine.

Conclusion

According to the results, materials with k-edges equal to energies common to diagnostic radiology can be proper substitutes for lead shields.

Keywords: Multi-Layered Shields, Diagnostic Radiology, Monte Carlo Simulation

1- Ray Medical Engineering Department, School of Mechanical Engineering, Shiraz University, Shiraz, Iran
*Corresponding author: Tel: +987136133640, E-mail: mehdizehtabian@yahoo.com

2- Radiation Research Center, School of Mechanical Engineering, Shiraz University, Shiraz, Iran

1. Introduction

As Low as Reasonably Achievable (ALARA) principle is of great significance in medical radiation protection. Radiation shielding aprons are commonly used for the protection of medical staff and patients against primary and scattered radiation during diagnostic imaging [1].

Lead is the most commonly used material in designing protective garments in diagnostic radiology. In fact, various studies have reported orthopedic traumas, caused by the weight of lead aprons [2, 3]. In addition, lead is a toxic substance and is recommended to be substituted if possible. Consequently, several researchers have recently attempted to design light lead-free radiation shields [1, 4-8].

Photon attenuation coefficients suddenly increase at K absorption edges. Therefore, radiation shields with k-edges equal to common energy exposures in radiology can be proper substitutes for lead shields. In this regard, Gaetano *et al.* evaluated three non-lead shields including EarthSafe, Xenolite and Demron. In their study, the attenuation performance of shields, which were almost 30% lighter than lead, was similar to lead itself [9].

McCaffrey *et al.* used EGs-nrc code to compare the attenuation coefficients of a pure lead sheet, two lead-based materials and three non-lead materials at 60-120 kVp X-ray energy ranges. As the results indicated, these materials resulted in similar or better radiation protection, compared to pure lead shields.

Moreover, Aghamiri *et al.* designed novel, flexible, lead-free shields against X-ray photons, used in diagnostic radiology via MCNP4c Monte Carlo simulations. According to the findings, the shield, composed of 55% tungsten (W) and 45% tin (Sn) in a polymer matrix, can be used as a low-weight non-lead shield [10].

Considering the abovementioned points, in the present study, we aimed to identify the best arrangement of heavy materials, *i.e.*, gadolinium (Gd), bismuth (Bi), barium (Ba), Sn and W, in shielding against X-rays and gamma rays used in radiology and nuclear medicine, respectively.

2. Materials and Methods

2-1- MCNP5 Monte Carlo code

MCNP5 Monte Carlo code, developed by Los Alamos National Laboratory (Los Alamos, New Mexico, USA), was used to perform the simulations in this research [11].

2-2- MCNP simulation

In this study, a well-collimated, mono-directional point source was simulated at a 50cm distance from cubical shields with $30 \times 30 \times 0.05 \text{ cm}^3$ dimensions. Cubic tally cells with $1 \times 1 \times 0.5 \text{ cm}^3$ dimensions were defined at a 5cm distance from the shields. The tally cells were also collimated to ensure proper geometrical condition. The schematic diagram of the simulation geometry is presented in Figure 1.

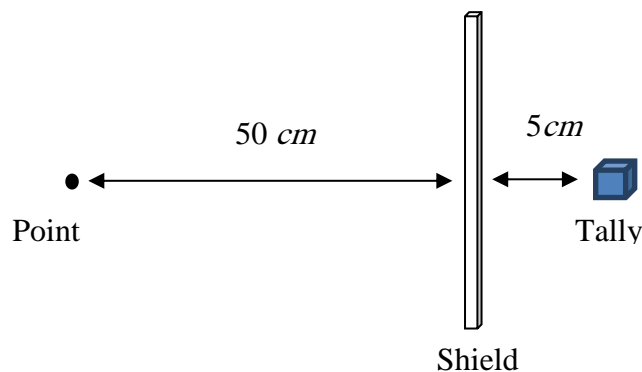


Figure 1. Geometry of simulation including the point source, shield and tally cell

The shielding properties of different materials at common energy ranges in radiology (i.e., 80 and 120 kVp) and ^{99m}Tc in nuclear medicine (140 keV gamma rays) were obtained. The energy spectra of 80 and 120 kVp X-rays were obtained from the IPEM report for a 1 mm aluminum filter at a node angle of 12° [12]. Tally types F4 and F5 were utilized to determine the flux and energy spectrum in tally cells, respectively. Considering the 10⁹ photon history, (nps= 10⁹), all simulations were performed in photon and electron modes to obtain a standard deviation less than 0.5%.

No variance reduction technique was applied in this study and no cut-off energy was considered for Monte Carlo simulations. Different single- and multi-layered aprons with a 0.5 mm thickness were simulated in this study (Figure 1). Moreover, the relative weights and photon attenuation properties of these shields were obtained relative to the 0.5 mm lead shield.

2-2-1- Single-layered shields

To compare the X-ray attenuation properties of materials mentioned in Table 1, single-layered shields, made up of each material, were simulated with 0.5 mm thickness.

Table 1. Elements used in the design of aprons

Materials	K absorption edge (keV)	Atomic number	Density (g/cm ³)
Barium (Ba)	37.4	56	3.5
Bismuth (Bi)	90.5	83	9.75
Gadolinium (Gd)	50.2	64	7.90
Lead (Pb)	88.0	82	11.36
Tin (Sn)	29.2	50	7.30
Tungsten (W)	69.5	74	19.3

Table 2. Different multi-layered shields simulated in this study

Layers	Shield arrangement	Thickness of each layer (mm)	Total Thickness (mm)
Two-layered shields	(Sn-Gd), (Gd-Sn), (Gd-W), (W-Gd), (Sn-W), (W-Sn), (Bi-Sn)	0.25	0.5
Three-layered shields	(Bi-Sn-Gd), (Gd-Sn-Bi), (W-Bi-Gd), (Gd-W-Bi)	0.167	0.5
Four-layered shields	(Sn-Ba-Gd-W), (W-Gd-Ba-Sn)	0.125	0.5
Five-layered shields	(Gd-Sn-Bi-W-Ba), (Ba-W-Bi-Sn-Gd)	0.1	0.5

2-2-2- Multi-layered shields

Based on the results of single-layered shields at 80 keV energy, different combinations of materials (two, three, four and five layers) were simulated with a total thickness of 0.5 mm (Table 2). The relative flux (F_{rel}) for each shield was obtained, using Equation 1:

$$F_{rel} = \frac{\text{Flux after 0.5mm of the shield}}{\text{Flux after 0.5mm lead}} \quad (1)$$

3. Results

3-1- Single-layered shields

The relative fluxes (F_{rel}) following the use of each shield at 80 kVp X-ray energy are demonstrated in Table 3. Also, the obtained X-ray spectra of the simulations following the use of each single-layered shield are shown in Figure 2.

Table 3 indicates the relative X-ray flux following the use of each shield against 120 kVp X-ray. The X-ray spectra after the use of single-layered shields are presented in Figure 3. Also, Table 3 demonstrates the relative X-ray flux following the utilization of each shield at 140 keV gamma -ray.

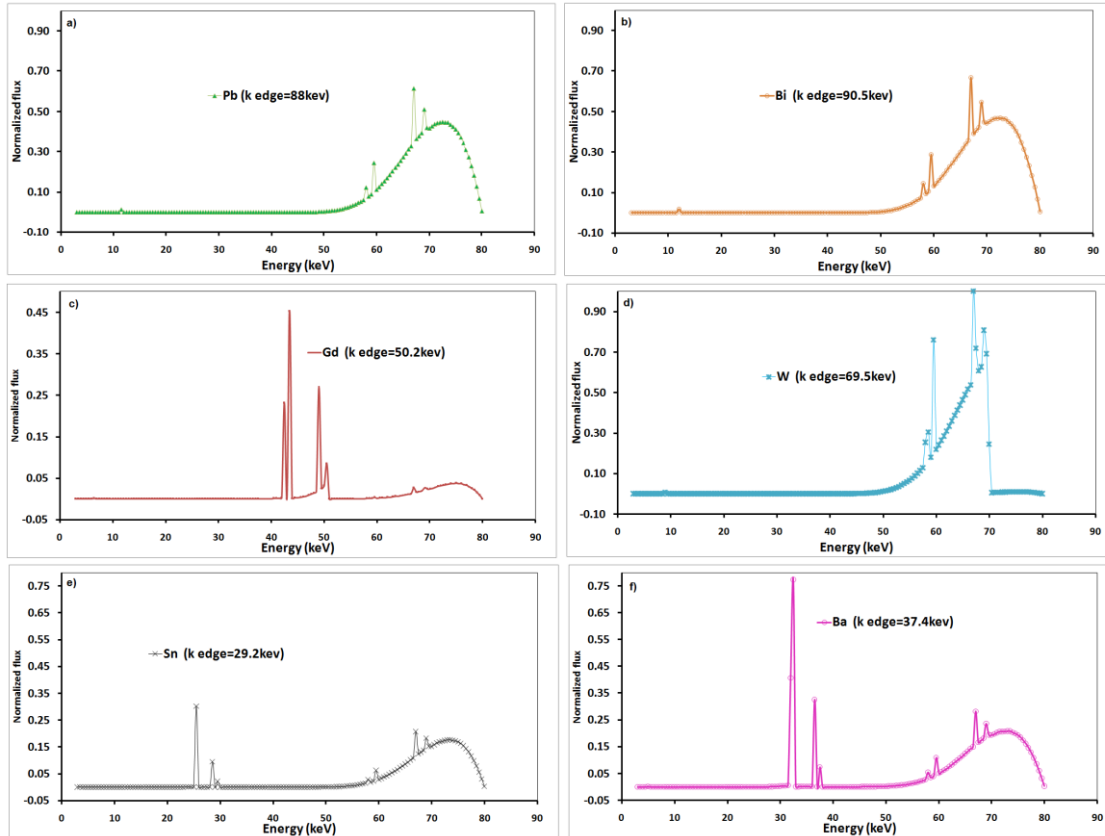


Figure 2. Normalized energy spectra after applying different multi-layered shields at 80 kVp X-ray energy: a) lead, b) bismuth, c) gadolinium, d) tungsten, e) tin, f) barium

Table 3. The total X-ray flux after using the shields, relative to the flux of lead shield at 80, 120 kVp X-ray energy, and 140 keV gamma rays.

Shield	F_{rel} 80 KV	F_{rel} 120 KV	F_{rel} 140 KV
W	0.64	0.24	0.64
Ba	0.95	5.86	3.08
Bi	0.92	1.32	1.43
Gd	0.09	1.30	2.28
Sn	0.54	2.06	2.92

3-1- Two-layered shields

As presented in Table 2, six two-layered shields were simulated in this study (i.e., Sn-Gd, Gd-Sn, Gd-W, W-Gd, Sn-W and W-Sn). Table 4 shows the total X-ray flux after applying the two-layered shields, compared to the flux following the use of lead shield.

3-2- Three-, four- and five-layered shields

The photon fluxes following the use of three-, four- and five-layered shields, compared to the flux of lead shield, are shown in tables 5, 6 and 7.

Shields with attenuations less than lead shields

Table 8 compares the properties (flux and weight) of all shields with $F_{rel} \leq 1$, with respect to the 0.5 mm lead shield. It should be mentioned that weight is considered for shields with 30×3

Table 4. The total X-ray flux after using two-layered shields relative to the flux following the use of lead

Shield	F_{rel} 80 kVp	F_{rel} 120 kVp	F_{rel} 140 keV
(Gd-Sn)	0.62	1.25	2.58
(Sn-Gd)	0.66	1.28	2.60
(Gd-W)	0.19	0.27	1.21
(W-Gd)	0.19	0.27	1.20
(Sn-W)	0.46	0.54	1.93
(W-Sn)	0.46	0.51	1.91

Table 5. The total X-ray flux after applying three-layered shields relative to the flux following the use of lead

Shield	F_{rel} 80kVp	F_{rel} 120kVp	F_{rel} 140keV
(Bi-Sn-Gd)	0.78	1.12	1.97
(Gd-Sn-Bi)	0.77	1.12	1.98
(Gd-W-Bi)	0.30	0.38	1.19
(W-Bi-Gd)	0.30	0.38	1.19

Light Multi-Layered Shields for Low Energy Photons

Table 6. The total X-ray flux after the use of four-layered shields, relative to the flux following the use of lead

Shield	F _{rel} 80kVp	F _{rel} 120kVp	F _{rel} 140keV
(Sn-Ba-Gd-W)	0.58	1.04	2.37
(W-Gd-Ba-Sn)	0.53	0.81	1.93

Table 7. The total X-ray flux after applying the shields relative to the flux of lead shield

Shield	F _{rel} 80kVp	F _{rel} 120kVp	F _{rel} 140keV
(Ba-W-Bi-Sn-Gd)	0.64	0.88	1.82
(Gd-Sn-Bi-W-Ba)	0.60	0.94	2.12

Table 8. Comparison of different shields with attenuations less than lead shields

Shield number	Shield layers	Energy	0.5 mm F _{rel}	0.5 mm shield weight/0.5 mm lead weight
1	Bi	80 kVp	0.92	0.86
2	W	80 kVp	0.64	1.07
		120 kVp	0.24	
		140 keV	0.64	
3	Sn	80 kVp	0.54	0.65
4	Ba	80 kVp	0.95	0.39
5	Gd	80 kVp	0.09	0.69
6	(Gd-Sn)	80 kVp	0.62	0.67
7	(Sn-Gd)	80 kVp	0.66	0.67
8	(Gd-W)	80 kVp	0.19	1.19
		120 kVp	0.27	
9	(Sn-W)	80 kVp	0.46	1.17
		120 kVp	0.54	
10	(W-Sn)	80 kVp	0.46	1.17
		120 kVp	0.50	
11	(W-Gd)	80 kVp	0.19	1.19
		120 kVp	0.27	
12	(Gd-W-Bi)	80 kVp	0.30	1.08
		120 kVp	0.38	
		140 kVp	1.19	
13	(W-Bi-Gd)	80 kVp	0.30	1.08
		120 kVp	0.38	
		140 kVp	1.19	
14	(Gd-Sn-Bi)	80 kVp	0.77	0.73
15	(Bi-Sn-Gd)	80 kVp	0.77	0.73
16	(W-Gd-Ba-Sn)	80 kVp	0.53	0.86
		120 kVp	0.81	
17	(Sn-Ba-Gd-W)	80 kVp	0.58	0.86
18	(Gd-Sn-Bi-W-Ba)	80 kVp	0.58	0.86
		120 kVp	0.94	
19	(Ba-W-Bi-Sn-Gd)	80 kVp	0.64	0.86
		120 kVp	0.88	
20	(Bi-W-Gd-Ba-Sn)	80 kVp	0.60	0.86

0×0.05 cm³ dimensions.

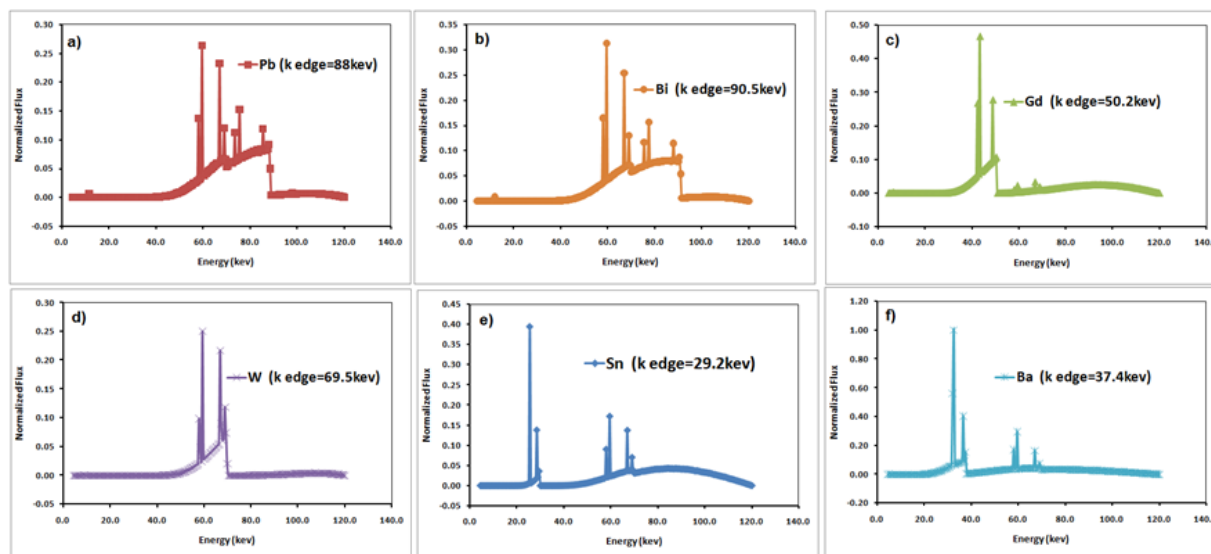


Figure 3. Normalized energy spectra after applying different multi-layered shields: a) lead, b) bismuth, c) gadolinium, d) tungsten, e) tin, f) barium

4. Discussion

4-1. Single-layered shields

According to Figure 2 and Table 3, gadolinium exhibited the best shielding efficiency among all materials in this study at 80 kVp X-ray energy. As presented in Table 3 and Figure 3, tungsten showed the most significant attenuation properties among all shields at 120 kVp X-ray energy. At 140 keV gamma rays, similar to 120 kVp energy, tungsten showed the best shielding efficiency among all shields.

4-2. Two-layered shields

According to the results presented in Table 4, Gd-W and W-Gd combinations exhibited the most significant attenuation properties among two-layered shields at 80 kVp and 120 kVp X-ray and 140 keV gamma ray energies.

4-3. Three-, four- and five-layered shields

According to table 5, among three-layered compositions, Gd-W-Bi and W-Bi-Gd shields showed the highest attenuation at three evaluated energy spectra. Among two four-layered shields, W-Gd-Ba-Sn showed better attenuation, as presented in Table 6. Also, according to Table 7, among five-layered shields, Ba-W-Bi-Sn-Gd composition showed better attenuation for the evaluated energy spectra.

4-4. The optimized shields for replacing lead aprons

As the comparison of different shields indicated, three-layered shields, composed of W-Bi-Gd, showed the best performance among all shields in this study at common energy ranges used in radiology and nuclear medicine (Table 9). This three-layered shield showed significant attenuation relative to lead at 80 kVp ($F_{rel}=0.30$) and 120 kVp ($F_{rel}=0.38$) energies, while the weight of the shield was almost similar to lead.

Table 9. The attenuation and weight of W-Bi-Gd shield relative to lead

Energy	Shield	F_{rel}	Weight
80 kVp		0.30	
120 kVp	W-Bi-Gd	0.38	1.08
140 keV		1.19	

5. Conclusion

The shielding properties of different non-lead materials were investigated at photon energies common in diagnostic radiology and nuclear medicine. Various single- and multi-layered shields, composed of barium, bismuth, gadolinium, tin and tungsten, were simulated, using Monte Carlo simulations in order to design environment-friendly shields, which are lighter than conventional lead aprons. According to the present findings, the three-

layered shield, composed of tungsten, bismuth and gadolinium, could be a proper substitute for lead in both diagnostic radiology and nuclear medicine.

References

1. Webster W. Experiments with medium Z materials for shielding against low-energy x-rays. *Radiology*, 1996; 86:146.
2. Klein LW, Miller DL, Balter S, Laskey W, Haines D, Norbash A, et al. Occupational health hazards in the interventional laboratory: time for a safer environment. *J Vasc Interv Radiol*. 2009 Jul;20(7 Suppl):S278-83.
3. Moore B, vanSonnenberg E, Casola G, Novelline RA. The relationship between back pain and lead apron use in radiologists. *AJR Am J Roentgenol*. 1992 Jan;158(1):191-3.
4. Webster EW. Addendum to 'Composite materials for x-ray protection'. *Health Phys*. 1991 Dec;61(6):917-8.
5. Zuguchi M, Chida K, Taura M, Inaba Y, Ebata A, Yamada S. Usefulness of non-lead aprons in radiation protection for physicians performing interventional procedures. *Radiat Prot Dosimetry*. 2008;131(4):531-4.
6. McCaffrey JP, Shen H, Downton B, Mainegra-Hing E. Radiation attenuation by lead and nonlead materials used in radiation shielding garments. *Med Phys*. 2007 Feb;34(2):530-7.
7. Takano Y, Okazaki K, Ono K, Kai M. Experimental and theoretical studies on radiation protective effect of a lighter non-lead protective apron. *Nihon Hoshasen Gijutsu Gakkai Zasshi*. 2005 Jul 20;61(7):1027-32.
8. Yaffe MJ, Mawdsley GE, Lilley M, Servant R, Reh G. Composite materials for x-ray protection. *Health physics*. 1991;60(5):661-4.
9. Scuderi GJ, Brusovanik GV, Campbell DR, Henry RP, Kwon B, Vaccaro AR. Evaluation of non-lead-based protective radiological material in spinal surgery. *Spine J*. 2006 Sep-Oct;6(5):577-82.
10. Aghamiri M, Mortazavi S, Tayebi M, Mosleh-Shirazi M, Baharvand H, Tavakkoli-Golpayegani A, et al. A Novel Design for Production of Efficient Flexible Lead-Free Shields against X-ray Photons in Diagnostic Energy Range. *Journal of Biomedical Physics and Engineering*. 2011;1(1 Dec).
11. Brown FB. MCNP—A General Monte Carlo N-Particle Transport Code, Version 5. Los Alamos National Laboratory, Oak Ridge, TN. 2003.
12. IPEM, Scientific Report Series No. 78, Catalogue of diagnostic x-ray and other spectra, Spectrum processor: IPEM Report 78 (CD_ROM). York: IPEM, 1997.